

Transport Properties of the Binary System L-(+)-Tartaric Acid–Water at 25 °C. A Velocity Correlation Study

Maria Castaldi, Gerardo D'Errico, Luigi Paduano, and Vincenzo Vitagliano*

Dipartimento di Chimica Dell'Università di Napoli, Federico II, Via Mezzocannone 4, 80134 Napoli, Italy

Accurate mutual diffusion and intradiffusion coefficients have been measured for the binary system L-(+)-tartaric acid (2)–water (1) at 25 °C. The collected diffusion coefficients have been combined with osmotic coefficients present in the literature to calculate the velocity correlation coefficients (VCC's). The results have been interpreted in terms of molecular interactions.

Introduction

This research is part of a program devoted to the study of equilibrium and transport properties of the quaternary system ethanol–glucose–L-(+)-tartaric acid–water, with the aim to test the theory that some of us developed in the past (Vitagliano et al., 1992), giving criteria for both static and dynamic gravitational stability of diffusion boundaries with four (or more) components. In the preliminary phase of this study we have been collecting a set of data on the corresponding binary and ternary systems. We have already analyzed the system glucose–water (Castaldi et al., 1998).

In this work, we remeasured densities for the binary system L-(+)-tartaric acid (2)–water (1) in the composition range approaching saturation. Furthermore, for the same system, we measured mutual diffusion and intradiffusion coefficients. These data are not present in the literature, to the authors' knowledge.

The data have been discussed in terms of velocity correlation coefficients (VCC's), that show how the macroscopic thermodynamic properties are affected by the solution structure at the molecular scale.

L-(+)-Tartaric acid is a weak diprotic acid [$K_1 = 9.268 \times 10^{-4} \text{ mol dm}^{-3}$ and $K_2 = 4.305 \times 10^{-5} \text{ mol dm}^{-3}$ (Robinson and Stokes, 1955)]. Figure 1 shows the fraction of the various species present in solution, computed using these K_i values, drawn as a function of the square root of the stoichiometric tartaric acid molality.

The experimental techniques allow an exhaustive examination in the region where the dissociated species concentration is not appreciable ($m > 0.09 \text{ mol kg}^{-1}$), although measurements were also made in the more dilute composition range.

Experimental Section

Materials. L-(+)-Tartaric acid purchased from Sigma Chemical Co. (99.5% purity) was used without further purification. All solutions were prepared by mass using double-distilled water. In all calculations the molecular weight of L-(+)-tartaric acid was assumed to be 150.1 g mol^{-1} .

Density Measurements. A set of density measurements were taken in the molality range 0–9 mol kg^{-1} with an Anton Paar 602 densimeter.

* Corresponding author. Fax: +39081 5527771. E-mail: Vita@chemna.dichi.unina.it.

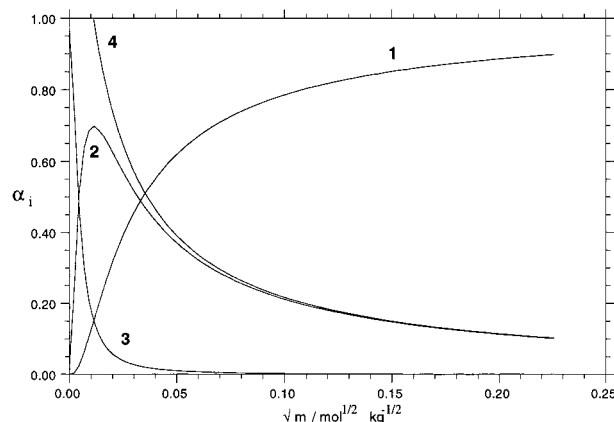


Figure 1. Fraction of the various species in aqueous solutions of L-(+)-tartaric acid as computed from the pK_a (Robinson and Stokes, 1955): **1**, AcH_2 ; **2**, AcH^- ; **3**, Ac^- ; **4**, H^+ .

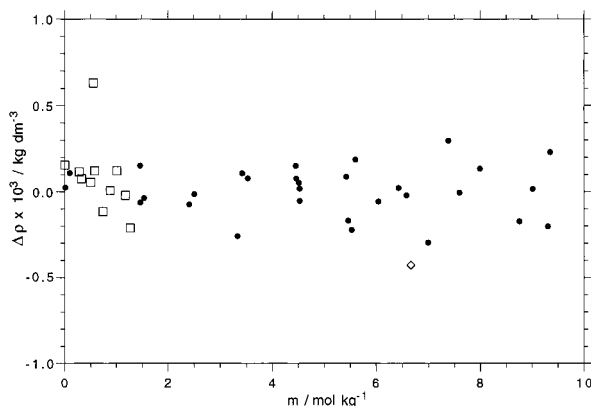
Table 1. Densities of Aqueous L-(+)-Tartaric Acid Solutions at 25 °C

$m/\text{mol kg}^{-1}$	$\rho/\text{kg dm}^{-3}$	$m/\text{mol kg}^{-1}$	$\rho/\text{kg dm}^{-3}$	$m/\text{mol kg}^{-1}$	$\rho/\text{kg dm}^{-3}$
0.0000	0.997 044	3.5241	1.170 85	6.0388	1.248 29
0.0069	0.997 53	4.4529	1.202 68	6.4237	1.258 14
0.0932	1.003 32	4.4577	1.202 76	6.5736	1.261 77
1.4587	1.082 76	4.5056	1.204 26	6.9892	1.271 32
1.4614	1.082 16	4.5215	1.204 74	7.3771	1.280 63
1.5343	1.085 77	4.5261	1.204 81	7.9845	1.293 31
2.4070	1.126 34	5.4207	1.231 70	8.7506	1.307 95
2.5067	1.130 67	5.4562	1.232 44	9.0057	1.312 86
3.3268	1.163 21	5.5239	1.234 28	9.2992	1.317 92
3.4218	1.167 12	5.5980	1.236 74	9.3445	1.319 16

The temperature of the densimeter was regulated at $(25.00 \pm 0.01) \text{ °C}$. For the densimeter calibration, air (at measured pressure and humidity) and distilled water, assumed density $0.997 044 \text{ kg dm}^{-3}$ (Lo Surdo et al., 1982), were chosen. The data, collected in Table 1, are in very good agreement with previous literature data (Thomsen, 1885; Dunstan and Thole, 1908). The experimental error is within $(1-2) \times 10^{-5} \text{ kg dm}^{-3}$. The coefficients of the polynomial equation fitted to the densities are given in Table 2. Figure 2 shows the deviation of experimental data from this equation. The limiting partial molar volume of undissociated L-(+)-tartaric acid was computed by interpolating the apparent molar volume of solute with a three-term polynomial, neglecting the first two experimental

Table 2. Coefficients of the Polynomial Equations Fitted to the Experimental Density and Diffusion Data ($=A_0 + A_1m + A_2m^2 + A_3m^3 + \dots \pm \sigma$)

	$\rho/\text{kg dm}^{-3}$	$10^5 D_{12}/\text{cm}^2 \text{ s}^{-1}$	$10^5 D_2^*/\text{cm}^2 \text{ s}^{-1}$	$10^5 D_1^*/\text{cm}^2 \text{ s}^{-1}$
A_0	0.997044	0.701 ± 0.013	0.798 ± 0.009	2.299
A_1	$(668.3 \pm 2.4) \times 10^{-4}$	$(-5.80 \pm 0.60) \times 10^{-2}$	-0.208 ± 0.010	-0.72 ± 0.02
A_2	$(-67.1 \pm 2.0) \times 10^{-4}$	$(1.13 \pm 0.57) \times 10^{-3}$	$(2.2 \pm 0.3) \times 10^{-2}$	0.102 ± 0.007
A_3	$(62.1 \pm 5.6) \times 10^{-5}$		$(-8 \pm 2) \times 10^{-4}$	$(-5.3 \pm 0.7) \times 10^{-3}$
A_4	$(-40.5 \pm 7.3) \times 10^{-6}$			
A_5	$(12.0 \pm 3.1) \times 10^{-7}$			
σ	1.4×10^{-4}	0.0105	0.0086	0.037

**Figure 2.** Comparison of L-(+)-tartaric acid aqueous solutions densities from different sources with eq 1: ●, our data; ◇, (Thomsen, 1885); □, (Dunstan and Thole, 1908).

data, referring to solutions in which dissociation was appreciable. The computed value is: $V_2^\infty(\text{AcH}_2) = 83.44 \pm 0.08 \text{ cm}^3 \text{ mol}^{-1}$.

Mutual Diffusion Coefficients. Mutual diffusion coefficients were measured with a Gouy diffusimeter (Gosting, 1950; Tyrrell and Harris, 1984) using a two-lens apparatus in which parallel light passing through a single-channel cell generates the fringe pattern on its focus. The initial boundary was formed with the siphoning technique. The light source was a Unifas PHASE 0.8-nW neon-helium laser operating at $\lambda = 632.8 \text{ nm}$. A Model "II fx" MacIntosh computer was used to control the scanning apparatus and to determine fringe positions from fringe intensity profiles.

The mutual diffusion coefficients D_{12} were calculated using a series of programs well described in the literature (Albright and Miller, 1989; Miller et al., 1992).

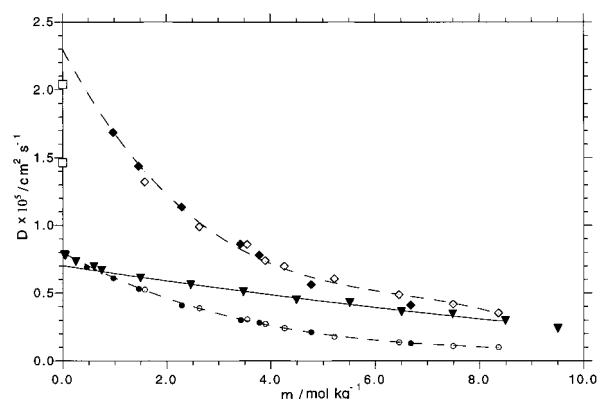
The experimental data, in the molality range 0–9 mol kg^{-1} , are collected in Table 3. The experimental error is within $(1-2) \times 10^{-3} \text{ cm}^2 \text{ s}^{-1}$. The coefficients of the polynomial equation fitted to the mutual diffusion coefficients in the molality range where the tartaric acid dissociation is negligible are given in Table 2. This equation was computed by least squares excluding the four diffusion data measured in the most diluted solutions where dissociation is appreciable. The experimental data and the polynomial trend are shown in Figure 3. The constant term, 0.701×10^{-5} , can be assumed as the limiting diffusion coefficient of undissociated tartaric acid, $D_{12}^\infty(\text{AcH}_2)$.

Intradiffusion Measurement. The intradiffusion measurements were made using the pulsed gradient spin-echo (PGSE) FT-NMR method (Stilbs, 1987; Callaghan, 1991; Weingärtner, 1994). Experiments were carried out on a Varian FT 80 NMR spectrometer operating in the ^1H mode, equipped with a pulsed magnetic field gradient unit, specially made by Stelar (Mede, Italy). The temperature was controlled to within $\pm 0.1 \text{ }^\circ\text{C}$ with a Stelar variable-temperature controller model VTC87. By using a pulse sequence where the echo delays are fixed and only the gradient pulse lengths are varied, the effects of relaxation

Table 3. Diffusion Data for the System L-(+)-Tartaric Acid–Water at 25 °C^a

$m/$ mol kg^{-1}	$\Delta m/$ mol kg^{-1}	J_m	$10^5 D_{12}/$ $\text{cm}^2 \text{ s}^{-1}$	$B(x_2)$	$10^5 D_T/$ $\text{cm}^2 \text{ s}^{-1}$
0.0000			1.171	1.000	1.171
0.0318	0.0623	45.46	0.783	1.004	0.779
0.0500	0.0862	62.16	0.776	1.007	0.771
0.2506	0.0602	40.01	0.731	1.035	0.706
0.6000	0.0719	51.40	0.695	1.086	0.640
0.7488	0.0605	37.31	0.669	1.108	0.603
1.4966	0.0755	41.49	0.612	1.222	0.501
2.4568	0.0997	45.65	0.560	1.371	0.409
3.4729	0.1023	39.94	0.511	1.524	0.335
4.4872	0.0687	21.64	0.451	1.663	0.271
5.5093	0.1773	55.56	0.429	1.782	0.241
6.4987	0.1499	36.66	0.363		
7.4841	0.2141	48.26	0.347		
8.4875	0.1604	32.25	0.298		
9.4992	0.1744	29.14	0.239		

^a m , average molality of each diffusion run. Δm , molality difference between bottom and top solutions. J_m , total number of Gouy fringes; in terms of the refractive index difference, Δn , (between the bottom and top solutions at the He–Ne laser red light ($\lambda = 632.8 \text{ nm}$), $J_m = (3.951 \times 10^6) \Delta n$). D_{12} , diffusion coefficients. $B(x_2)$, thermodynamic factor. D_T , thermodynamic diffusion coefficient.

**Figure 3.** Comparison of mutual diffusion and intradiffusion coefficients of aqueous L-(+)-tartaric acid solutions at 25 °C: ◇, D_1^* in light water; ◆, D_1^* in heavy water; ○, D_2^* in light water; ●, D_2^* in heavy water; ▼, D_{12} ; □, computed limiting mutual diffusion coefficients of monodissociated and bidissociated species.

are constant and need not be taken into consideration. The spin-echo peak amplitudes for a given line follow the equation

$$I = I_0 \exp \left[-\frac{2\tau}{T_2} - \gamma^2 g^2 D_i^* \delta^2 \left(\Delta - \frac{\delta}{3} \right) \right] \quad (1)$$

where γ is the gyromagnetic ratio of the nucleus, D_i^* is the intradiffusion coefficient of molecules, g is the gradient strength, δ and Δ are the length and spacing of the gradient pulses, τ is the time lag between pulses at 90° and 180° , and T_2 is the spin-spin relaxation time, respectively.

The PGSE-NMR method requires the presence of a deuterated substance as reference, in the measurement region. For aqueous solutions two different methods have been alternatively used. In the first method the measurements were carried out on solutions prepared with undeuterated solvent, using the coaxial tubes (Wilma model WGS-5BL) with C_6D_6 as external reference and lock. In dilute solutions, the water signal can be so strong it hinders the other ones.

The second method used D_2O as solvent. This procedure, enhancing the signal intensity of the solute, allows us to analyze very dilute solutions. On the other hand it introduces some errors owing to the isotope effects on the intradiffusion rate. In this case a correction is needed to obtain the corresponding values in light water. Hertz (Goldammer and Hertz, 1970) proposed to multiply the experimental results measured in D_2O by the factor 1.23, which is the ratio of intradiffusion coefficients of normal and deuterated water, as well as the reciprocal of the ratio of their viscosities. In principle, this correction neglects the possible differences in the interactions of these two solvents with the solute. In fact, D_2O is thought to be slightly more structured than H_2O (Nemethy and Scheraga, 1964), so that the hydrophobic effect and the formation of hydrogen bonds could be favored. As a consequence, the ratio of solute intradiffusion coefficients in D_2O and H_2O can also depend on the solute nature and concentration.

The two different techniques were applied with the aim of testing the correctness of this correction for the L-(+)-tartaric acid–water system. A good agreement was found between the two sets of measurements. A single polynomial interpolated both sets of experimental data. The polynomial coefficients are reported in Table 2.

In the same measurement sets D_{OH}^* values were determined. Since the proton exchange between L-(+)-tartaric acid OH's and water is much faster than the single spin-echo sequence, the D_{OH}^* value is a mean value that can be split between L-(+)-tartaric acid and water contributions according to the expression

$$D_{OH}^* = \frac{4m}{4m + (2 \times 55.5)} D_2^* + \frac{2 \times 55.5}{4m + (2 \times 55.5)} D_1^* \quad (2)$$

where $m/\text{mol kg}^{-1}$ is the L-(+)-tartaric acid molality. This equation allows us to compute D_1^* . The measured values of D_{OH}^* , D_2^* , and the computed D_1^* are collected in Table 4 a and b. The experimental error is within $(1-2) \times 10^{-2} \text{ cm}^2 \text{ s}^{-1}$. The D_1^* data obtained from the two experimental sets fit a polynomial whose coefficients are collected in Table 2. Figure 3 shows the experimental D_1^* and D_2^* data and the interpolating equations.

Experimental Results

In binary systems, the diffusive transport is described by the flux equation

$$J_2 = -M_2 \text{ grad } \mu_2 \quad (3)$$

correlating the flow J_2 , expressed in the mass-fixed reference frame, to the chemical potential μ_2 ; M_2 is the mobility that describes the actual tendency of molecules to diffuse.

Considering the difficulty of treating with the chemical potential gradient, we prefer Fick's phenomenological equation:

$$J_2 = -D_{12} \text{ grad } C_2 \quad (4)$$

Table 4. Intradiffusion Data on the System L-(+)-Tartaric Acid–Water at 25 °C

$m/$ mol kg^{-1}	x_2	$10^5 D_{OH}^*/$ $\text{cm}^2 \text{ s}^{-1}$	$10^5 D_1^*/$ $\text{cm}^2 \text{ s}^{-1}$	$10^5 D_2^*/$ $\text{cm}^2 \text{ s}^{-1}$
(a) Measured in D_2O and Multiplied by the Factor 1.23				
0.0000	0.0000	2.299	2.299	
0.4568	0.0091			0.69
0.9716	0.0191	1.71	1.69	0.61
1.1632	0.0285	1.47	1.44	0.53
2.2841	0.0438	1.17	1.13	0.41
3.4195	0.0641	0.90	0.86	0.30
3.7815	0.0704	0.82	0.78	0.27
4.7659	0.0872	0.60	0.56	0.21
6.6794	0.1180	0.44	0.41	0.13
(b) Measured in H_2O				
0.0000	0.0000	2.299	2.299	
1.5779	0.0303	1.35	1.32	0.53
2.6237	0.0494	1.03	0.99	0.39
3.5455	0.0656	0.90	0.86	0.31
3.8944	0.0716	0.78	0.74	0.25
4.2577	0.0777	0.74	0.70	0.24
5.2125	0.0935	0.64	0.60	0.18
6.4501	0.1132	0.52	0.48	0.14
7.4924	0.1292	0.45	0.42	0.11
8.3580	0.1420	0.39	0.41	0.10

The diffusion coefficient D_{12} can be obtained multiplying M by the thermodynamic term B , accounting for the fact that the actual diffusion driving force is not the concentration gradient but the chemical potential gradient:

$$D_{12} = M_2 B_2 \quad (5)$$

The thermodynamic factor B is correctly expressed in a molar concentration scale:

$$B(C_2) = RT \left(1 + \frac{d \ln y_2}{d \ln C_2} \right) \quad (6)$$

y_2 being the activity coefficient expressed as a function of molarity.

In this paper we prefer to express the thermodynamic term $B(x)$ as a function of mole fraction, according to the Laity notation (Laity, 1959):

$$B(x_2) = \left(1 + \frac{d \ln f_2}{d \ln x_2} \right) = \left(1 + \frac{d \ln f_1}{d \ln x_1} \right) = B(x_1) \quad (7)$$

where x_i and f_i are the mole fraction and rational activity coefficient of component i , respectively. In this way a unique mobility term is defined $M_2 = M_1 = D_T$, called the thermodynamic diffusion coefficient.

The thermodynamic factor was straightforwardly computed by differentiating the logarithm of solvent activity, $\ln a_1$, obtained from literature osmotic data (Robinson et al., 1942), with respect to $\ln x_1$, where x_1 is the stoichiometric water mole fraction.

The term $B(x_2)$ was well fitted by the equation

$$B(x_2) = 1 + 7.20x_2 + 53.4x_2^2 - 411x_2^3 \pm 0.01 \quad (0.02 < x_2 < 0.09) \quad (8)$$

The limiting diffusion coefficients at infinite dilution for the ionic species can be computed with the Nernst–Hartley equation from the literature equivalent conductivity data

(Vanysek, 1993), $\lambda_+^{\circ} = 349.65$ and $\lambda_-^{\circ} = 59.6 \text{ m}^2 \text{ S mol}^{-1} \times 10^4$

for the second dissociation: $D_{12}^{\infty}(\text{Ac}^{2-}) =$

$$(2.662 \times 10^{-7}) \frac{3\lambda_+^{\circ}\lambda_-^{\circ}}{2\lambda_+^{\circ}\lambda_-^{\circ}} = 2.033 \times 10^{-5} \text{ cm}^2 \text{ s}^{-1} \quad (9)$$

for the 1st dissociation: $D_{12}^{\infty}(\text{AcH}^-) =$

$$(2.662 \times 10^{-7}) \frac{\lambda_+^{\circ}\lambda_-^{\circ}}{\lambda_+^{\circ} + (\lambda_-^{\circ}/2)} = 1.462 \times 10^{-5} \text{ cm}^2 \text{ s}^{-1} \quad (10)$$

and for the intradiffusion: $D_2^{*\infty} =$

$$(2.662 \times 10^{-7}) \frac{\lambda_-^{\circ}}{2} = 0.794 \times 10^{-5} \text{ cm}^2 \text{ s}^{-1} \quad (11)$$

where the mobilities of Ac^{2-} and AcH^- were assumed to be equal. The extrapolated $D_2^{*\infty}$ obtained from our NMR data (Table 2) is in perfect agreement with the value given in eq 11.

An attempt was made to correlate our mutual diffusion data with the values that could be computed in the very dilute solutions.

For the ionized species we assumed the following approximate expression:

$$D_i = D_i^{\infty} \left(1 + \Delta_1 \left(1 + \frac{\partial \ln y_{\pm}}{\partial \ln C} \right) \right) \quad (12)$$

where we used, for the thermodynamic term, the expression

$$\left(1 + \frac{\partial \ln y_{\pm}}{\partial \ln C} \right) = 1 - \frac{1.1722|z_+z_-|\sqrt{I}}{2(1 + 2\sqrt{I})^2} \quad (13)$$

and, for the Onsager correction term, the expression

$$\Delta_1 = -\frac{0.4351\sqrt{I}}{1 + 2\sqrt{I}} \quad (14)$$

where I is the ionic strength computed on the basis of the actual concentrations of the various ions.

The diffusion coefficient of the solution is given, at each molality, by the expression (Robinson and Stokes, 1955)

$$D_{12} = \alpha_{\text{Ac}^{2-}} D_{12}(\text{Ac}^{2-}) + \alpha_{\text{AcH}^-} D_{12}(\text{AcH}^-) + \alpha_{\text{AcH}_2} D_{12}(\text{AcH}_2) \quad (15)$$

where the α_i values are the fractions of each species present at the given molalities and D_{AcH_2} was taken from the polynomial whose coefficients are reported in Table 2.

Equation 15 is quite approximate; however, a good agreement was found in the range of overlapping between experimental and computed values. This can be seen in Figure 4.

Discussion

Mutual diffusion coefficients D_{12} and thermodynamic diffusion coefficients D_T are shown in Figure 5 drawn as a function of the solute mole fraction.

Inspection of Figure 5 shows that both mutual and thermodynamic diffusion coefficients decrease with the mole fraction of solute, while the thermodynamic factors increase with x_2 (Table 2). This gives evidence that the mobility contribution prevails on ruling the behavior of diffusion coefficients. An opposite effect can be found in

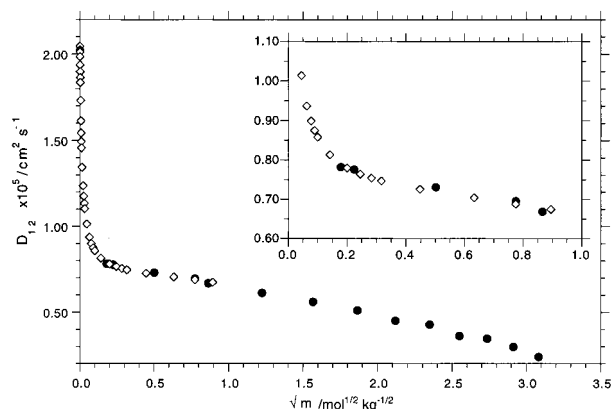


Figure 4. Mutual diffusion coefficients of tartaric acid: ●, experimental data; ◇, computed data (see text).

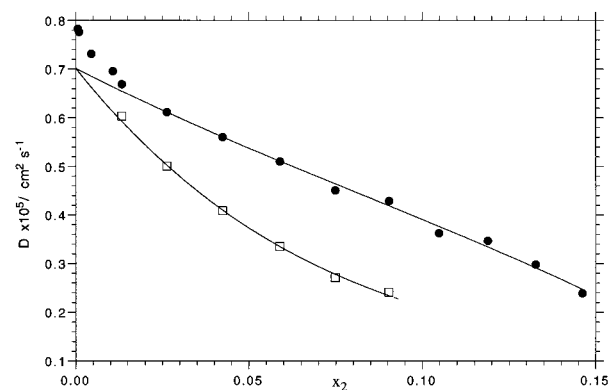


Figure 5. Diffusion coefficients (●) and thermodynamic diffusion coefficients (□) of L-(+)-tartaric acid aqueous solutions at 25 °C.

some systems, such as surfactant solutions, where both thermodynamic and diffusion coefficients decrease with solute concentration, while mobilities increase (Leaist, 1986; Paduano et al., 1997).

Computing the velocity cross-correlation coefficients, VCC's (McCall and Douglass, 1967; Mills and Hertz, 1980), a deeper insight into the system characteristics can be obtained. VCC's are more sensitive to specific interactions than the experimental diffusion coefficients and allow an analysis from the microscopic point of view (Weingärtner, 1990; Ambrosone et al., 1995).

The phenomenological coefficients can be expressed in terms of time integrals over velocity correlation functions, which give access to a more direct kinetic interpretation of observed physical quantities.

The intradiffusion coefficient D_i^* of component i can be defined as (Steele, 1969)

$$D_i^* = \frac{1}{3} \int_0^{\infty} \langle v_s^i(0) \cdot v_s^i(t) \rangle dt \quad (16)$$

where the v_s^i is the velocity of a single particle numbered s of component i at time 0 and t , respectively. The pointed brackets indicate the ensemble average.

The velocity correlation coefficients reflect the correlation in the motion of two different particles s and r :

$$f_{ij} = \frac{N}{3} x_j \int_0^{\infty} \langle v_s^i(0) \cdot v_r^j(t) \rangle dt \quad (17)$$

where N is the total number of particles in the system. Equation 17 characterizes the correlation motion between different particles of the same or of different components.

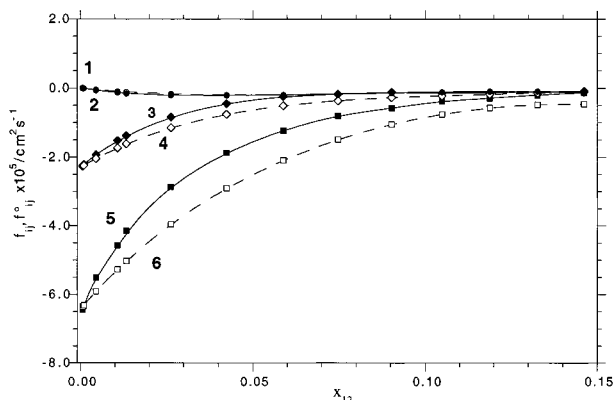


Figure 6. Velocity cross-correlation factors for the system L-(+)-tartaric acid–water at 25 °C: **1**, f_{22} ; **2**, f_{22}^e ; **3**, f_{11} ; **4**, f_{11}^e ; **5**, f_{12} ; **6**, f_{12}^e .

The VCC's can be expressed as a function of the experimental quantities D_1^* , D_2^* , and D_{12} (McCall and Douglass, 1967)

$$f_{12} = -D_{12} \frac{M_1 M_2}{(x_1 M_1 + x_2 M_2)^2 B(x_1)} x_2 \quad (18)$$

$$f_{ij}^e = D_{12} \frac{M_j^2 x_j}{(x_1 M_1 + x_2 M_2)^2 B(x_1)} - D_i^* \quad (19)$$

where M_i is the molecular weight of component i and $B(x_1)$ is the thermodynamic factor in the mole fraction scale, as defined by eq 7.

According to Hertz's (1982) approach, formulas for standard velocity cross correlation coefficients f_{ij}^e can be derived, by using the law of effective linear momentum conservation and applying the ideal mixing rule:

$$f_{12}^e = - \frac{M_1 x_2}{(x_1 M_1 + x_2 M_2)} D_1^* (1 + x_1 P_{12}) \quad (20)$$

$$f_{ii}^e = - \frac{M_i x_i}{(x_1 M_1 + x_2 M_2)} D_i^* (1 - x_j P_{ij}) \quad (21)$$

where

$$P_{ij} = \frac{M_j D_j^*}{M_i D_i^*} - 1 \quad (22)$$

The quantities f_{ij}^e are representative of a fictitious ideal reference system formed by non-interacting components; in their computation the mutual diffusion coefficient, accounting for the global motion of the species in the system, is not involved. The relationship between the f_{ij} and f_{ij}^e coefficients play the role of indicator for the molecular association effects. As discussed in detail elsewhere (Mills and Hertz, 1980; Weingärtner, 1990), molecular association should lead to more correlated motions than those expected for an "ideal" system. The general association criterion is

$$f_{ij} > f_{ij}^e \quad (23)$$

The VCC's and the corresponding standard correlation coefficients are reported in Figure 6.

Inspection of Figure 6 shows that f_{22} coincides almost exactly with f_{22}^e , which implies, according to eq 23, that there is no self-association between L-(+)-tartaric acid molecules.

On the contrary the interactions L-(+)-tartaric acid–water and water–water appear to be sensible.

The existence of the interaction water–water is suggested by the observation that f_{11} is larger than the corresponding f_{11}^e .

Furthermore, according to the results shown in Figure 6, the interaction between L-(+)-tartaric acid and water seems to be the larger effect. This interaction is reflected in the behavior of f_{12} : in fact $f_{12} \gg f_{12}^e$ in the whole range of explored concentration, stressing the presence of strong cross-associations between solute and water.

These evidences can be imputed to the strong hydrophilic behavior of L-(+)-tartaric acid, whose molecule can form hydrogen bonds with water. The solvent molecules participating in the L-(+)-tartaric acid hydration shell interact strongly among themselves, thus explaining the enhanced water–water interactions.

Literature Cited

- Albright, G. J.; Miller, D. G. Non linear regression programs for the analysis of Gouy fringe patterns from isothermal free-diffusion experiments for three-component systems. *J. Phys. Chem.* **1989**, *93*, 2169–2175.
- Ambrosone, L.; D'Errico, G.; Sartorio, R.; Vitagliano, V. Analysis of velocity cross-correlation and preferential solvation for the system *N*-methylpyrrolidone–water at 20 °C. *J. Chem. Soc., Faraday Trans.* **1995**, *91*, 1339–1344.
- Callaghan, P. T. *Principles of Nuclear Magnetic Resonance Microscopy*; Clarendon Press: Oxford, U.K., 1991.
- Castaldi, M.; D'Errico, G.; Paduano, L.; Vitagliano, V. Transport properties of binary system glucose–water at 25 °C. A velocity correlation study. *J. Chem. Eng. Data* **1998**, *43* (3), 653–657.
- Dunstan, A. E.; Thole, F. B. The Relation between Viscosity and Chemical constitution. Part II. The existence of Racemic Compounds in the Liquid State. *J. Chem. Soc.* **1908**, *93*, 1815–1825.
- Goldammer, E. V.; Hertz, H. G. Molecular motion and structure of aqueous mixtures with nonelectrolyte as studied by nuclear magnetic relaxation methods. *J. Phys. Chem.* **1970**, *74*, 3734–3755.
- Gosting, J. L. A Study of the Diffusion of Potassium Chloride in water at 25 °C with the Gouy Interference Methodology. *J. Am. Chem. Soc.* **1950**, *72*, 4418–4422.
- Hertz, H. G. Momentum conservation determining diffusion in binary molecular and electrolyte solutions. *Z. Phys. Chem., Suppl.* **1982**, *1*, 7–40.
- Laity, R. W. An application of irreversible thermodynamics to the study of diffusion. *J. Phys. Chem.* **1959**, *63*, 80–83.
- Leaist, D. G. Binary diffusion of micellar electrolytes. *J. Colloid Interface Sci.* **1986**, *111*, 230–239.
- Lewis, N. G.; Randall, M. *Thermodynamics*, 2nd ed.; McGraw-Hill: New York 1961.
- Lo Surdo, A.; Alzola, E. M.; Millero, F. J. The (p, V, T) properties of concentrated aqueous electrolytes. I. Densities and apparent molar volumes of NaCl, Na₂SO₄, MgCl₂, and MgSO₄ solutions from 0.1 mol kg⁻¹ to saturation from 273.15 to 323.15 K. *J. Chem. Thermodyn.* **1982**, *14*, 649–662.
- McCall, D. W.; Douglass, D. C. Diffusion in Binary Solution. *J. Phys. Chem.* **1967**, *71*, 987–997.
- Miller, D. G.; Sartorio, R.; Paduano, L. An extrapolation procedure to obtain the total fringe number from Gouy fringe pattern data. *J. Solution Chem.* **1992**, *21*, 459–476.
- Mills, R.; Hertz, H. G. Application of the Velocity Cross-Correlation Method to Binary Nonelectrolyte Mixtures. *J. Phys. Chem.* **1980**, *84*, 220–224.
- Nemethy, G.; Scheraga, H. A. Structure of water and hydrophobic bonding in proteins. IV. The thermodynamic properties of liquid deuterium oxide. *J. Chem. Phys.* **1964**, *41*, 680–689.
- Paduano, L.; Sartorio, R.; Vitagliano, V.; Costantino, L. Equilibrium and transport properties of aqueous penta ethylenglycol 1-hexyl ether and sodium hexanesulfonate at 25 °C. *J. Colloid Interface Sci.* **1997**, *189*, 189–198.
- Robinson, R. A.; Smith, P. K.; Smith, E. R. B. The osmotic coefficients of some organic compounds in relation to their chemical constitution. *Trans. Faraday Soc.* **1942**, *38*, 63–70.
- Robinson, R. A.; Stokes, R. H. *Electrolyte Solutions*; Butterworth: London, 1955.
- Steele, W. A. In *Transport Phenomena in Fluids*; Hanley, H. J. M., ed.; Marcel Dekker: New York, 1969; Chapter 8.
- Stilbs, P. Fourier transform pulsed-gradient spin-echo studies of molecular diffusion. *Prog. Nucl. Reson. Spectrosc.* **1987**, *19*, 1–45.
- Thomsen, T. Analysis of Equilibrium properties in aqueous solutions. *J. Prakt. Chem.* **1885**, *32*, 211–230.

- Tyrrell, H. J.; Harris, K. R. *Diffusion in Liquids*; Butterworth: London, 1984.
- Vanysek, P. In *Handbook of Chemistry and Physics*, 74th ed.; CRC Press: Boca Raton, FL, 1993; pp 5–90.
- Vitagliano, P. L.; Ambrosone, L.; Vitagliano, V. Gravitational instabilities in multicomponent free diffusion boundaries. *J. Phys. Chem.* **1992**, *96*, 1431–1437.
- Weingärtner, H. The Microscopic Basis of intra-diffusion-Mutual diffusion Relationship in Binary Liquid Mixtures. *Ber. Bunsen-Ges. Phys. Chem.* **1990**, *4*, 358–364.

Weingärtner, H. *NMR Studies of self-diffusion in liquids*; The Royal Society of Chemistry, Annual Reports, Section C; The Royal Society of Chemistry: Herts, U.K., 1994; pp 37–69.

Received for review November 25, 1998. Accepted March 10, 1999. This research was carried out with the financial support of Italian M.U.R.S.T. (Cofin.97 CFSIB) and of Italian C.N.R.

JE980295K